Dynamically Stable Helices of Poly(*N*-propargylamides) with Bulky Aliphatic Groups

Jianping Deng, Junichi Tabei, Masashi Shiotsuki, Fumio Sanda, and Toshio Masuda*

Department of Polymer Chemistry, Graduate School of Engineering, Kyoto University, Kyoto 615-8510, Japan

Received April 7, 2004; Revised Manuscript Received May 11, 2004

ABSTRACT: *N*-Propargylamides with bulky pendent groups [$HC{\equiv}CCH_2NHCOR$, **9**: R = $CH_2C(CH_3)_3$, **10**: R = $C(CH_3)_3$, **11**: R = $C(CH_3)_2CH_2CH_2CH_3$, **12**: R = $CH(CH_2CH_3)_2$, **13**: R = $CH(CH_2CH_2CH_3)_2$] were polymerized with a rhodium catalyst, $(nbd)Rh^+B^-(C_6H_5)_4$ (nbd = 2,5-norbornadiene), to obtain the polymers in 80−92% yields. Poly(**11**) and poly(**12**) possessed moderate molecular weights ($M_n \geq 10\,000$) and were totally soluble in a few solvents including chloroform. On the other hand, the M_n values of poly(**9**), poly(**10**), and poly(**13**) were no more than 5000, and these polymers were not completely soluble in any solvents. The conformational transition behavior of these polymers was examined by temperature-variable UV−vis spectroscopy in chloroform solution, which revealed that poly(**10**)−poly(**13**) could form dynamically stable helical conformation even at 60 °C. By copolymerizations of monomers **9** and **10** with monomer **4**, $HC{\equiv}CCH_2NHCO(CH_2)_4H$, the solubility of the polymers was effectively improved and almost all the copolymers totally dissolved in chloroform, while the molecular weights of the copolymers increased up to 18 600−45 000. Moreover, the helix contents of poly($\mathbf{4}_{0.63}$-*co*-$\mathbf{9}_{0.37}$) and poly($\mathbf{4}_{0.40}$-*co*-$\mathbf{10}_{0.60}$) were the highest among the two series of (co)polymers, respectively. It is concluded that the copolymerization of **9** and **10** with **4** effectively decreased the steric repulsion between the crowded side chains, which probably allowed the copolymers to take helical conformation efficiently.

Introduction

In recent years, synthetic helical polymers have drawn growing attention, and a number of significant achievements have been made in this field.[1] Synthetic helical polymers remind us the stable helical conformation of naturally occurring biomacromolecules, such as proteins and DNA. The helical senses of proteins are generally predetermined by the chiral information contained in the sequence of amino acids. The helices of proteins are usually stabilized by intramolecular hydrogen bonds. Generally speaking, it is unfavorable for biomacromolecules to take stable helical conformation from the viewpoint of entropy; nevertheless, the enthalpy of the formation of hydrogen bonds compensates it. Stimulated by this strategy of nature, polymer chemists have tentatively designed and synthesized polymers which can form intramolecular hydrogen bonding with the hope to obtain polymers which are able to form stable helices.[1] Unfortunately, it still remains difficult that nonconvalent interactions such as hydrogen bonds govern the secondary structure of synthetic polymers. Indeed, success has been made only in a few special oligomers and polymers.[1]

We have designed and synthesized two kinds of polyacetylenes, poly(propiolic esters)[2] and poly(*N*-propargylamides),[3] which can form dynamically stable helical conformation under certain conditions. The driving forces with which they form helices are different from each other. Steric repulsion contributes to the formation of helices in the former polymers,[2] while in the latter, the intramolecular hydrogen bonding between the neighboring amide groups in the side chain plays a predominant role so that the latter polymers can take helical conformation.[3] In our preceding study,[4] some poly(*N*-propargylamides) with pendent groups of various lengths [poly(**1**)−poly(**8**) in Scheme 1] were synthesized, and their secondary structures were investigated by UV−vis spectroscopy. Poly(*N*-propargylamides) with pendent groups of medium lengths [(poly(**5**) and poly(**6**)] could take relatively stable helices at room temperature.[4] In contrast, the other polymers hardly took helical conformation at room temperature. Low stereoregularity may be responsible in polymers with long side chains [poly(**7**) and poly(**8**)], whereas the bulkiness of pendent group does not seem enough for the formation of helices in polymers with short alkyl chains [poly(**2**)−poly(**4**)].[4] The stereoregularity and higher order structure of poly(**1**) could not be determined because of its insolubility.

Nevertheless, all the helices formed in poly(**2**)−poly(**8**) were more or less unstable at high temperature. More specifically, all these polymers took random coil conformation instead of helix upon raising temperature up to 27 °C and above. Improvement of the stability of helical structure in these polymers is not only interesting from the viewpoint of synthesis of novel helical polymers but also important from the viewpoint of application of the helical polymers to chiral separating materials. The present study deals with the polymerization of five *N*-propargylamides with bulky pendent groups, **9**−**13** (Scheme 1), and the elucidation of the conformational transition behavior of the formed polymers by UV−vis spectroscopy. We also examine the copolymerizations of either monomer **9** or **10** with monomer **4**, on one hand, to keep the helix-forming ability of poly(**9**) and poly(**10**) and, on the other hand, to improve the solubility of poly(**9**) and poly(**10**) and increase the molecular weights.

---

* Corresponding author: Tel +81-75-383-2589; Fax +81-75-383-2590; e-mail masuda@adv.polym.kyoto-u.ac.jp.

10.1021/ma049321b CCC: $27.50 © 2004 American Chemical Society
Published on Web 06/15/2004

Scheme 1

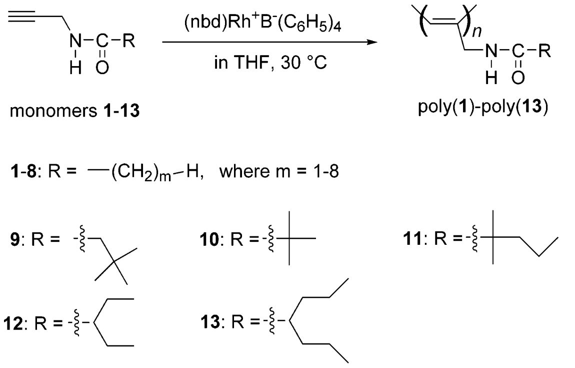

Experimental Section

Measurements. Melting points (mp) were measured by a Yanaco micro melting point apparatus. The molecular weights and molecular weight distributions of (co)polymers were determined by GPC (Shodex KF-850 column) calibrated by using polystyrene as standards and THF or chloroform as an eluent. IR spectra were recorded with a Shimadzu FTIR-8100 spectrophotometer. Elemental analysis was carried out at the Kyoto University Elemental Analysis Center. UV–vis spectra were recorded on a JASCO J-820 spectropolarimeter. ^{1}H and ^{13}C NMR spectra were recorded on a JEOL EX-400 spectrometer.

Materials. THF as polymerization solvent was distilled by the usual method. Propargylamine (TCI), *tert*-butylacetic acid (TCI), pivalic acid (TCI), 2,2-dimethyl-*n*-valeric acid (TCI), 2-ethyl-*n*-butyric acid (TCI), 2-propyl-*n*-valeric acid (TCI), thionyl chloride (Wako), pyridine (Wako), isobutyl chloroformate (Wako), and 4-methylmorpholine (Wako) were used as received without further purification. The (nbd)Rh^{+}B^{-}(C$_6$H$_5$)$_4$ catalyst was prepared as reported.[5]

Monomer Synthesis. Monomers **4** and **10** were synthesized according to the method reported in the preceding article.[4a] Monomers **9** and **11**–**13** were synthesized according to the method introduced earlier.[3a] Monomers, **10**, **11**, and **13** were new compounds. Now, taking the synthesis of monomers **10** and **11** as examples, the main synthetic procedures of the two different methods are described. Monomer **10** (Scheme S1 in the Supporting Information): pivalic acid (5.6 mL, 49.0 mmol), isobutyl chloroformate (6.4 mL, 49.0 mmol), and 4-methylmorpholine (5.4 mL, 49.0 mmol) were added to THF (200 mL) sequentially. The solution was stirred at room temperature for 10 min, and then propargylamine (3.4 mL, 49.0 mmol) was added to the solution. After 1 h, white precipitate formed was filtered off, and the filtrate was collected, to which ethyl acetate (ca. 50 mL) was added to extract the desired product. The combined solution was washed with 2 N HCl three times and then washed with saturated aqueous NaHCO$_3$ to neutralize the solution. Then, the solution was dried over anhydrous MgSO$_4$, filtered, and concentrated to give the target monomer. The crude monomer was further purified by flash column chromatography on silica gel (hexane/AcOEt = 2/1, v/v). Monomer **11** (Scheme S2 in the Supporting Information): 2,2-dimethyl-*n*-valeric acid (5.0 mL, 35.0 mmol) was added to thionyl chloride (1.3 mL, 17.5 mmol), and then the solution was refluxed. After 1 h, ethyl ether (200 mL), pyridine (2.8 mL, 35.0 mmol), and propargylamine (2.4 mL, 35.0 mmol) were added sequentially to the solution. The solution was stirred at 0 °C for 2 h, and then the white precipitate formed was filtered off. The filtrate was washed with 2 N HCl three times and then with saturated aqueous NaHCO$_3$ to neutralize the solution. Afterward, the solution was dried over anhydrous MgSO$_4$, filtered, and concentrated to give the target monomer. The crude monomer was further purified twice by flash column chromatography on silica gel (hexane/AcOEt = 3/1, v/v). Monomers **9**, **12**, and **13** were prepared similarly to monomer **11** from the corresponding carboxylic acids. The data of monomers **10**, **11**, and **13** were as follows:

Table 1. Polymerization of Monomers 9–13[a]

monomer	yield[b] (%)	M_n[c]	M_w/M_n[c]
9	92[d]	4000	1.06
10	80[d]	3100	2.57
11	86	10000	1.64
12	89	19000	3.14
13	90[d]	2300	3.24

[a] With (nbd)Rh^{+}B^{-}(C$_6$H$_5$)$_4$ catalyst in THF at 30 °C for 1 h; $[M]_0 = 1.0$ M; $[M]_0/[Rh] = 100$. [b] Precipitated in hexane. [c] Measured by GPC (polystyrenes as standards; chloroform as eluent). [d] Partly soluble in THF (65%) and CHCl$_3$ (70%).

Monomer **10**: yield 35%, colorless crystal, mp 58–60 °C. IR (KBr): 3290 (H–N), 2928, 2360 (H–C≡), 1641 (C=O), 1550, 1460, 1261, 1211, 1010, 655, 626, 559 cm^{-1}. ^{1}H NMR (CDCl$_3$, 400 MHz, 20 °C): δ 1.18–1.58 [–C(*CH*$_3$)$_3$], 2.20–2.25 (*CH*≡C), 4.00 –4.05 (CH≡C*CH*$_2$), 5.70–5.80 (N*H*).^{13}C NMR (CDCl$_3$, 400 MHz, 20 °C): δ 20.79, 27.47, 29.46, 56.24, 71.61, 74.50, 185.56. Anal. Calcd for C$_8$H$_{13}$NO: C, 69.03; H, 9.41; N, 10.06. Found: C, 68.82; H, 9.63; N, 9.94. Monomer **11**: yield 25%, colorless liquid, bp 129–131 °C (760 mmHg). IR (KBr): 3292 (H–N), 2370 (H–C≡), 1641 (C=O), 1545, 1425, 1277, 1118, 696, 667, 632, 569 cm^{-1}. ^{1}H NMR (CDCl$_3$, 400 MHz, 20 °C): δ 0.81–0.89 (CH$_2$CH$_2$*CH*$_3$), 1.12–1.30 [C(*CH*$_3$)$_2$, *CH*$_2$CH$_3$), 1.40–1.50 (*CH*$_2$CH$_2$CH$_3$), 2.15–2.20 (*CH*≡C), 3.95–4.05(CH≡C*CH*$_2$), 5.80 –5.85 (N*H*).^{13}C NMR (CDCl$_3$, 400 MHz, 20 °C): δ 14.54, 17.99, 25.24, 29.29, 42.05, 43.59, 71.41, 79.83, 177.47. Anal. Calcd for C$_{10}$H$_{17}$NO: C, 71.81; H, 10.25; N, 8.37. Found: C, 71.87; H, 10.50; N, 8.14. Monomer **13**: yield 45%, colorless crystal, mp 47–49 °C. IR (KBr): 3295 (H–N), 2932 (H–C≡), 1632 (C=O), 1541, 1232, 1122, 675, 553, 490 cm^{-1}. ^{1}H NMR (CDCl$_3$, 400 MHz, 20 °C): δ 0.89–1.05 (CH$_2$CH$_2$*CH*$_3$), 1.60–1.65 (CH$_2$*CH*$_2$CH$_3$), (2.05–2.21 (*CH*≡C, *CH*$_2$C$_2$H$_5$), 4.03–4.10 (CH≡C*CH*$_2$), 5.55–5.68 (N*H*).^{13}C NMR (CDCl$_3$, 400 MHz, 20 °C): δ 14.12, 19.02, 20.80, 29.01, 35.19, 47.52, 71.51, 72.37, 186.52. Anal. Calcd for C$_{11}$H$_{19}$NO: C, 72.88; H, 10.56; N, 7.73. Found: C, 72.62; H, 10.76; N, 7.69.

Polymerization and Copolymerization. (Co)polymerizations were carried out with (nbd)Rh^{+}B^{-}(C$_6$H$_5$)$_4$ as a catalyst in dry THF at 30 °C for 1 h under the following conditions: [monomer]$_0$ = 1.0 M, [catalyst] = 10 mM. After polymerization, the reaction mixture was poured into a large amount of hexane to precipitate the formed (co)polymer. Then, the (co)polymer was filtered off, washed with hexane, and dried under reduced pressure. In the case of copolymerization, the total monomer concentration was kept 1.0 M, while other conditions were the same as for homopolymerization.

Results and Discussion

Synthesis and Helical Conformation of Homopolymers. Table 1 shows that monomers **11** and **12** underwent polymerization smoothly to give polymers having moderate molecular weights ($M_n \geq 10\,000$) in good yields (ca. 90%). However, polymerizations of other three monomers **9**, **10**, and **13** just provided oligomers under the same conditions, whose molecular weights were lower than 5000. The reason should be probably the low solubility of these oligomers in THF. Poly(**12**) dissolved in chloroform, THF, and toluene smoothly, while poly(**11**) dissolved totally in chloroform but only partly in THF and toluene (Table S1 in the Supporting Information). The solubility of other three oligomers was not satisfactory; i.e., they only partly dissolved in chloroform, CH$_2$Cl$_2$, and THF and hardly dissolved in 1,2-dichloroethane, chlorobenzene, *o*-dichlorobenzene, toluene, DMF, DMSO, and methanol. The ^{1}H NMR spectra of the polymers/oligomers recorded in CDCl$_3$ at 50 °C exhibited broad olefinic proton signals, which prevented us from determining the cis contents of the main chains.

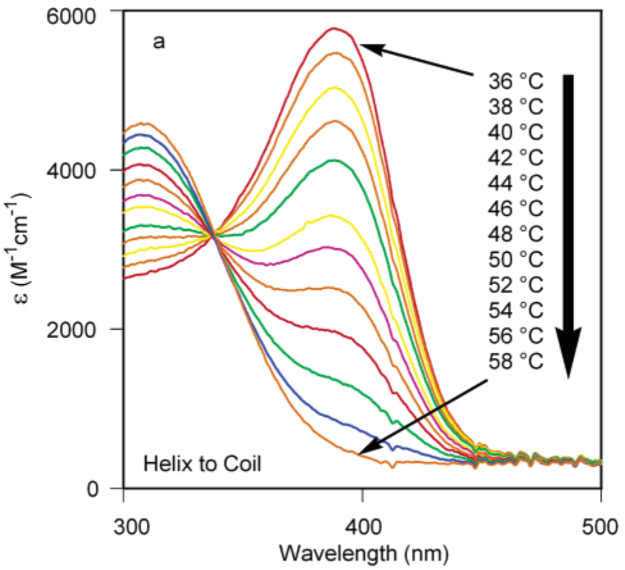

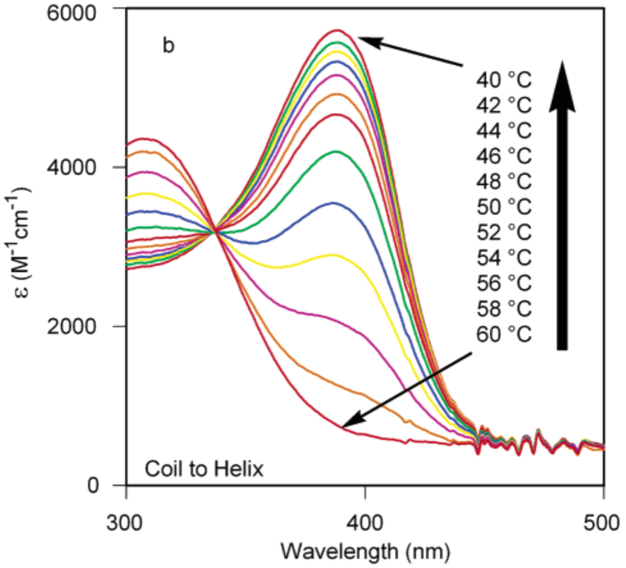

Figure 1. Temperature dependence of UV−vis spectra of poly(**9**) (c = 0.10 mM measured in $CHCl_3$).

As we had previously reported,[3] poly(N-propargylamides) with appropriate pendent groups could take helical conformation owing to hydrogen bonding intramolecularly formed between the amide groups in the side chains. Using the part soluble in chloroform, the secondary structure of the polymers/oligomers synthesized in the current study was investigated by recording UV−vis spectra at different temperatures, which had been proved to be a simple and effective method to study the secondary structure of poly(N-propargylamides).[3,4] Applying this UV−vis methodology, we can conclude that poly(**9**) exists predominantly in helical conformation below 36 °C because only one strong absorption peak was observed at about 390 nm in the UV−vis spectrum (Figure 1a). When the temperature was raised to 38 °C, the conformational transition from helix to random coil began to take place. With further increasing temperature, the absorption intensity of the peak at 390 nm continued to weaken, while the absorption intensity at 320 nm became gradually stronger, which reflects the helix-to-coil transition of the polymer. When the temperature reached 58 °C, the absorption peak at 390 nm completely disappeared and the peak at 320 nm took a maximum. This means that the helix-to-coil transition was completed at 58 °C and that the polymer predominantly took a random coil conformation above this temperature. Figure 1b shows the change of UV−vis spectrum with decreasing temperature. When the temperature was lowered, the coil-to-helix transition began at 58 °C and the transition process lasted down to 40 °C. It is concluded from Figure 1 that poly(**9**) can form helices at about 40−60 °C higher temperatures than poly(**5**) and poly(**6**) which have been studied in the preceding articles.[4]

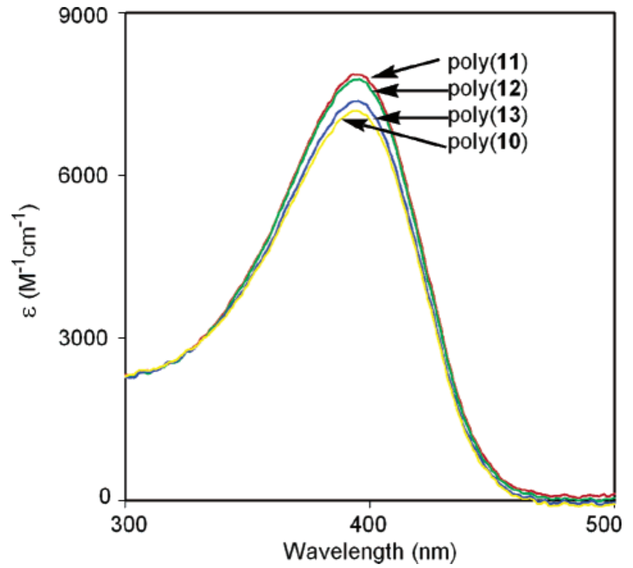

Figure 2. UV−vis spectra of poly(**10**)−poly(**13**) (c = 0.10 mM measured in $CHCl_3$ at 60 °C). The data of poly(**10**) and poly(**13**) were approximately determined because they were partly (30%) insoluble in $CHCl_3$.

Figure 2 presents the UV−vis spectra of poly(**10**)−poly(**13**) measured at 60 °C. It should be further described that all the UV−vis spectra in Figure 2 hardly changed below 60 °C compared to those at 60 °C. According to the UV−vis spectra in Figure 2, all these polymers/oligomers can form helices even at 60 °C, which is evidenced by the strong absorption peak at 390 nm and the absence of the peak at 320 nm. By comparing these polymers/oligomers with those studied earlier,[4] it can be concluded that the steric repulsion between the bulky pendent groups also make a large contribution to the formation of helices in addition to the hydrogen bonding intramolecularly formed between the amide groups.

Synthesis and Helical Conformation of Poly(4-*co*-9). The polymers/oligomers studied in the present research are interesting since they can form helices at relatively high temperature. However, the low solubility of poly(**9**), poly(**10**), and poly(**13**) is a drawback, resulting in difficult analysis of their higher order structure by UV−vis spectroscopy. Aiming at detailed investigation of the secondary structure of these polymers, copolymerization was attempted to improve the solubility of the polymers.

Copolymerization of monomers **4** and **9** was carried out, whose results are given in Table 2. These monomers smoothly copolymerized to provide copolymers with moderate M_n's in high yields. The compositions of the resulting copolymers were determined from their ^1H NMR spectra by calculating the relative peak intensity of protons in $-C{\equiv}C-CH_2-$ (4 ppm) to all the protons in the alkyl groups (0.8−2.5 ppm). The compositions of

Table 2. Copolymerization of Monomers 4 and 9[a]

monomer feed (**4**/**9**, mol/mol)	yield[b] (%)	M_n[c]	M_w/M_n[c]	**4** in copolymer[d] (mol %)	cis[d] (%)
0/100	92[e]	4000	1.06	0	n.d.[f]
20/80	93[e]	7600	8.41	21	100
40/60	90	16000	1.99	42	100
60/40	89	18600	1.38	63	99
80/20	87	9200	2.11	79	100
100/0	80	9500	2.32	100	98

[a] With (nbd)$Rh^+B^-(C_6H_5)_4$ catalyst in THF at 30 °C for 1 h; $[M]_0 = 1.0$ M; $[M]_0/[Rh] = 100$. [b] Precipitated in hexane. [c] Measured by GPC (polystyrenes as standards; chloroform as eluent except for the monomer feed **4**/**9** = 100/0, where THF was used). [d] Determined by ^1H NMR in $CDCl_3$ at 50 °C. [e] Partly soluble in THF and $CHCl_3$. [f] Cis content could not be determined because the olefinic proton signal was too broad.

the copolymers were almost identical to those of the corresponding monomer feeds. The solubility of the copolymer containing 21% unit **4** was not effectively improved compared to the homopolymer of **9**; i.e., it dissolved only partly in common organic solvents. In contrast, when the content of monomer **4** was 42% and above, the solubility of the copolymers was satisfactory. The copolymers had high stereoregularity; namely, their cis contents were almost quantitative.

The secondary structure of these (co)polymers was investigated by UV–vis spectroscopy. The UV–vis absorption at 390 nm was the strongest in poly($\mathbf{4}_{0.63}$-*co*-$\mathbf{9}_{0.37}$) among the copolymers of **4** and **9**. The UV–vis spectrum of poly($\mathbf{4}_{0.63}$-*co*-$\mathbf{9}_{0.37}$) is presented in Figure 3 for the sake of comparison with those of poly(**9**) (Figure 1) and poly(**4**).[4] To discuss the conformational transition behavior of polymers, several temperatures are defined as follows: T_1 and T_2 are the temperatures at which the coil-to-helix transition begins and ends, and T_3 and T_4 are the temperatures at which the helix-to-coil transition begins and ends, respectively. The helix content at T_1 and T_4 is zero, whereas the helix content at T_2 and T_3 is not necessarily 100% but is a maximum for each (co)polymer under the given conditions. T_1 and T_2 of these (co)polymers are given in Figure 4a and T_3 and T_4 in Figure 4b. Figure 4a indicates that poly(**4**) begins to form helical conformation at −13 °C and that this coil-to-helix transition process lasts down to −40 °C. When temperature was raised again, the polymer reversibly underwent helix-to-coil transition (Figure 4b). This transition process ranged from −37 °C (T_3) to −11 °C (T_4).[4a] Poly(**9**) started to undergo a helix-to-coil transition at 36 °C, which ended at 58 °C. It showed coil-to-helix transition in the temperature range from 60 to 40 °C (Figure 1). In the copolymers composed of monomers **4** and **9**, all of T_1−T_4 were located between those of the corresponding homopolymers. Take poly($\mathbf{4}_{0.63}$-*co*-$\mathbf{9}_{0.37}$) for example. T_1−T_4 were 20, −14 (Figure 3b), −12, and 24 °C (Figure 3a), respectively.

Among these (co)polymers, poly($\mathbf{4}_{0.63}$-*co*-$\mathbf{9}_{0.37}$) showed the largest UV–vis absorption at 390 nm (Figure 3). Hence, the UV–vis absorption intensities of other (co)polymers relative to that of this copolymer [poly($\mathbf{4}_{0.63}$-*co*-$\mathbf{9}_{0.37}$)] were calculated by the method employed in the preceding articles,[4] whose result is depicted in Figure 5. The relative intensities of poly(**4**) and poly(**9**) were 52% and 63%, respectively. With increase of the content of unit **4** in the copolymers, the relative intensity of $\epsilon_{390\ nm}$ of the copolymers gradually increased, and then it drastically decreased when the content of unit **4** in the copolymer exceeded 63%. These results imply that the copolymers could form helical conformation more easily compared to both of the homopolymers, poly(**4**) and poly(**9**). It is likely that the bulkiness of the pendent group of poly(**4**) is not enough to induce a helix efficiently. On the other hand, it is assumed for poly(**9**) as follows: the pendent groups may be too bulky, and hence the large steric repulsion between the pendent groups possibly will have an adverse effect on the formation of hydrogen bonding that generates a stable helix. It seems that an exquisite balance for the formation of helical structure is satisfactorily achieved in the copolymer poly($\mathbf{4}_{0.63}$-*co*-$\mathbf{9}_{0.37}$) to provide the helical structure more readily than both poly(**4**) and poly(**9**) do.

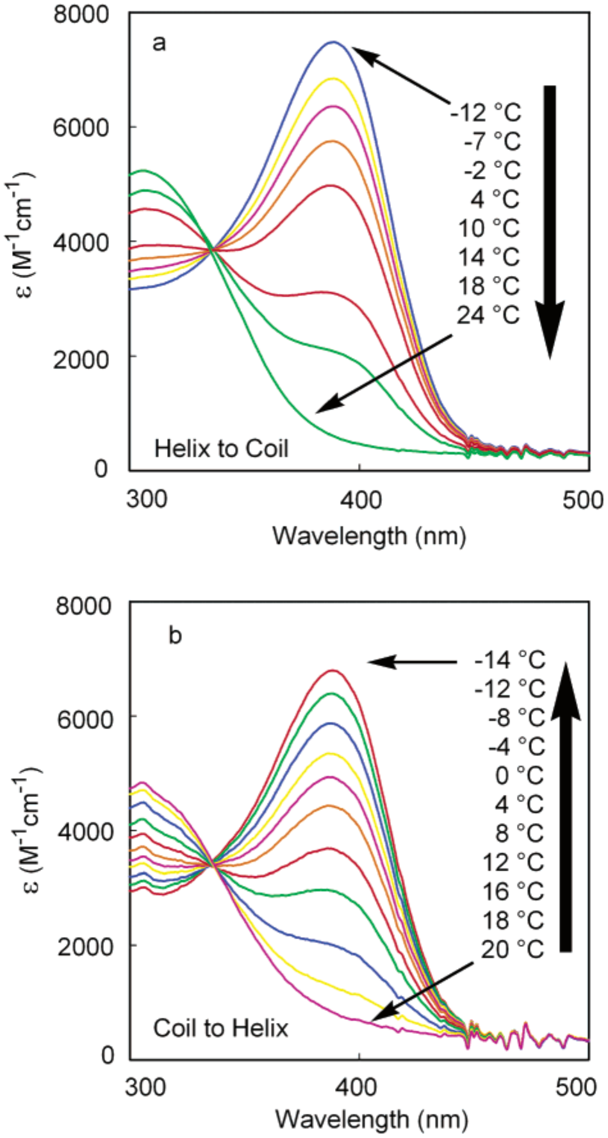

Figure 3. Temperature dependence of UV–vis spectra of poly($\mathbf{4}_{0.63}$-*co*-$\mathbf{9}_{0.37}$) (c = 0.10 mM measured in $CHCl_3$).

Thermodynamic parameters, i.e., ΔH (change in enthalpy), ΔS (change in entropy), and ΔG (change in free energy), for the coil-to-helix transition of these (co)polymers were determined by the method described earlier,[4] and the data are deployed in Figure 6. Both ΔH and ΔS became larger in negative sign with increasing unit **4** in the copolymers, and they took maximum values at 63% of unit **4** and 37% of **9**. This finding agrees well with the results observed in Figure 5, where poly($\mathbf{4}_{0.63}$-*co*-$\mathbf{9}_{0.37}$) showed a maximum UV–vis absorption. Thus, it is concluded that the formation of the helix is accompanied by large decreases in ΔH

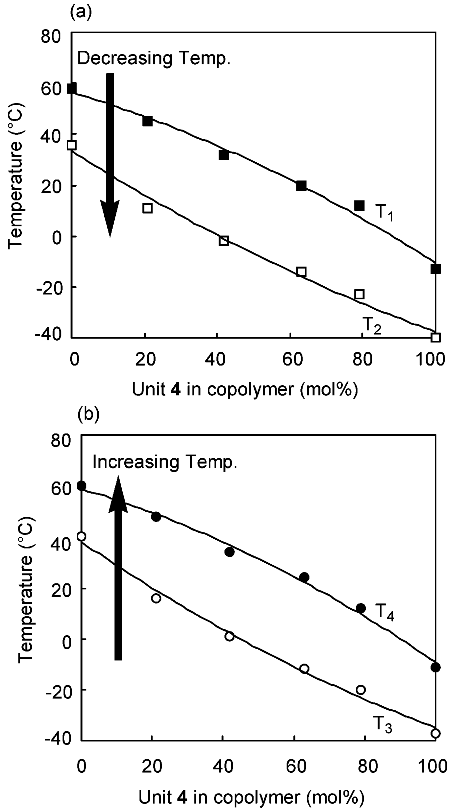

Figure 4. Temperature dependence of conformational transition of poly(**4**-*co*-**9**)s ($c = 0.10$ mM measured in $CHCl_3$). T_1 and T_2 are the temperatures at which the coil-to-helix transition begins and ends, respectively; T_3 and T_4 are the temperatures at which the helix-to-coil transition begins and ends, respectively.

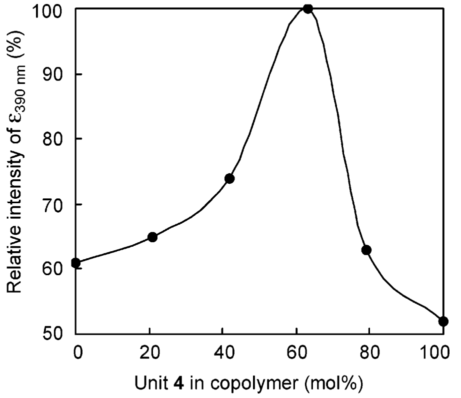

Figure 5. Effect of copolymer composition on the relative intensity of ϵ at 390 nm of poly(**4**-*co*-**9**)s determined by UV–vis spectroscopy measured in $CHCl_3$ ($c = 0.10$ mM) at −45 °C.

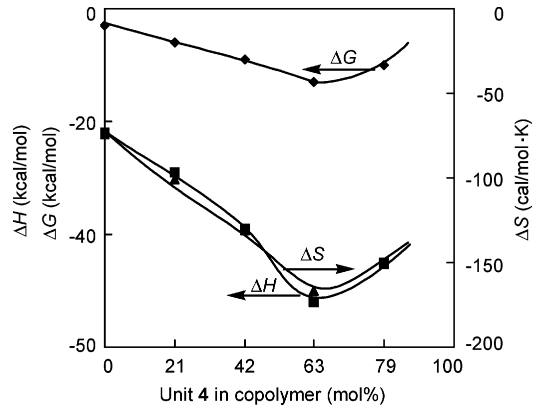

Figure 6. Plots of ΔH, ΔS, and ΔG (at −45 °C) vs composition of poly(**4**-*co*-**9**)s.

Table 3. Copolymerization of Monomers 4 and 10[a]

monomer feed (**4**/**10**, mol/mol)	yield[b] (%)	M_n[c]	M_w/M_n[c]	cis[d] (%)
0/100	80[e]	3 100	2.57	n.d.[f]
20/80	100[e]	20 000	1.37	n.d.[f]
30/70	98	33 000	1.93	n.d.[f]
40/60	99	45 000	1.88	n.d.[f]
50/50	100	19 400	2.89	100
60/40	100	15 000	3.19	100
80/20	96	11 250	4.03	100
100/0	80	9 500	2.32	98

[a] With $(nbd)Rh^+B^-(C_6H_5)_4$ catalyst in THF at 30 °C for 1 h; $[M]_0 = 1.0$ M; $[M]_0/[Rh] = 100$. [b] Precipitated in hexane. [c] Measured by GPC (polystyrenes as standards; THF as eluent except for the monomer feed **4**/**10** = 100/0, where THF was used). [d] Determined by ^1H NMR in $CDCl_3$ at 50 °C. [e] Partly soluble in THF and $CHCl_3$. [f] Cis content could not be determined because the olefinic proton signal was too broad.

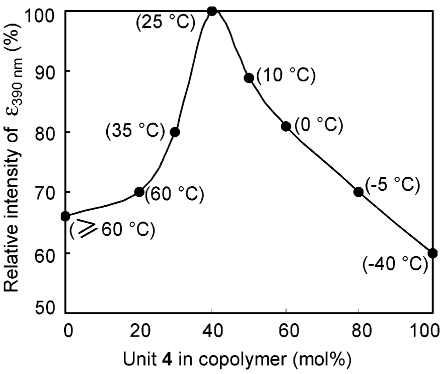

Figure 7. Effect of copolymer composition on the relative intensity of ϵ at 390 nm of poly(**4**-*co*-**10**)s determined by UV–vis spectroscopy measured in $CHCl_3$ ($c = 0.10$ mM) at −45 °C. In the parentheses, the temperatures at which the (co)polymers began to take the helix-to-coil transition are shown.

and ΔS, which seems to be reasonable from the viewpoint of thermodynamics. In addition, poly($\mathbf{4}_{0.63}$-*co*-$\mathbf{9}_{0.37}$) gave the largest ΔG with negative sign, providing the evidence for reasoning that poly($\mathbf{4}_{0.63}$-*co*-$\mathbf{9}_{0.37}$) formed the most stable helix among the assessed (co)polymers.

Synthesis and Helical Conformation of Poly(4-*co*-10). Table 3 shows that the copolymerizations of monomers **4** and **10** also proceed smoothly to afford the corresponding copolymers with moderate M_n's in high yields. When the content of unit **4** in the copolymers was 30% and above, the copolymers totally dissolved in chloroform. When the content of unit **4** in the copolymer exceeded 50%, the cis contents of the copolymers were quantitative. However, when the content of unit **4** was lower than 50%, the cis contents could not be determined because the signals assigned to the olefinic protons were very broad.

The secondary structure of the copolymers was examined by UV–vis spectroscopy measured in chloroform. The (co)polymers hardly underwent a helix-to-coil transition below 60 °C, indicating that the helices of these (co)polymers are dynamically stable at this temperature range. The relative intensities of UV–vis absorption at 390 nm of the (co)polymers at −45 °C are plotted against the compositions of the (co)polymers using the value of poly($\mathbf{4}_{0.40}$-*co*-$\mathbf{10}_{0.60}$) as a standard (Figure 7). In the figure, the temperatures at which the (co)polymers start undergoing a helix-to-coil conforma-

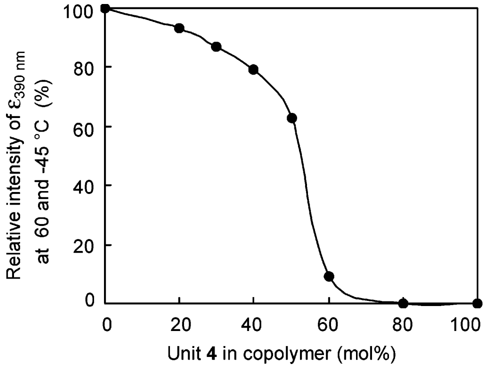

Figure 8. Effect of copolymer composition on the ratio of the $\epsilon_{390\ \mathrm{nm}}$ values at 60 and −45 °C of poly(**4**-*co*-**10**)s determined by UV−vis spectroscopy measured in $CHCl_3$ (c = 0.10 mM).

tional transition upon raising temperature are shown in parentheses. We can observe similar results to those in Figure 5. The temperature dependence of the helix-to-coil conformational transition of these (co)polymers was similar to that in Figure 4b.

As the temperature was raised, the helix content of these (co)polymers gradually decreased. The relative $\epsilon_{390\ \mathrm{nm}}$ of these (co)polymers at 60 °C to the corresponding $\epsilon_{390\ \mathrm{nm}}$ at −45 °C is illustrated in Figure 8. Poly(**10**) kept the same $\epsilon_{390\ \mathrm{nm}}$ at 60 °C as that at −45 °C. The ratio of ϵ at 60 and −45 °C gradually decreased as the unit of **4** increased. When the content of unit **4** exceeded 50%, the ratio of ϵ at 60 and −45 °C abruptly decreased. The relative $\epsilon_{390\ \mathrm{nm}}$ of poly($\mathbf{4}_{0.60}$-*co*-$\mathbf{10}_{0.40}$) was no more than about 10%. Poly($\mathbf{4}_{0.80}$-*co*-$\mathbf{10}_{0.20}$) and poly(**4**) existed in random coil conformation at 60 °C. On the basis of these results, it can be concluded that the copolymerization not only improved the solubility of the copolymers effectively and increased the molecular weight largely but also adjusted the stability and content of helix, when the copolymer composition was tuned.

Conclusions

N-Propargylamides with bulky pendent groups (**9**−**13**) were synthesized. Monomers **11** and **12** satisfactorily underwent polymerization with Rh catalyst to give polymers with moderate molecular weights and good solubility in chloroform. On the other hand, monomers **9**, **10**, and **13** provided only oligomers under the given polymerization conditions, presumably because of the low solubility of the products. Poly(**10**)−poly(**13**) could form helices even at 60 °C. By copolymerization of either **9** or **10** with **4** which contains linear alkyl group, the solubility of the copolymers could be improved effectively. In addition, the composition and temperature dependence of the conformational transition behavior of these copolymers were clearly observed. Poly($\mathbf{4}_{0.63}$-*co*-$\mathbf{9}_{0.37}$) and poly($\mathbf{4}_{0.40}$-*co*-$\mathbf{10}_{0.60}$) exhibited the highest helix contents among poly(**4**-*co*-**9**)s and poly(**4**-*co*-**10**)s, respectively. Cooperational effects of hydrogen bonding and steric repulsion were observed for the process of helix formation.

Supporting Information Available: Solubility of poly(**9**)−poly(**13**) and synthetic schemes of monomers **10** and **11**. This material is available free of charge via the Internet at http://pubs.acs.org.

References and Notes

(1) For the synthetic helical polymers, see: (a) Yashima, E.; Maeda, K.; Nishimura, T. *Chem.*−*Eur. J.* **2004**, *10*, 42−51. (b) Nakano, T.; Okamoto, Y. *Chem. Rev.* **2001**, *101*, 4013−4038. (c) Green, M. M.; Park, J.-W.; Sato, T.; Teramoto, A.; Lifson, S.; Selinger, R. L. B.; Selinger, J. V. *Angew. Chem., Int. Ed.* **1999**, *38*, 3138−3154. (d) Rowan, A. E.; Nolte, R. J. M. *Angew. Chem., Int. Ed.* **1998**, *37*, 63−68. (e) Pu, L. *Acta Polym.* **1997**, *48*, 116−141. (f) Okamoto, Y.; Nakano, T. *Chem. Rev.* **1994**, *94*, 349−372. (g) Nolte, R. J. M. *Chem. Soc. Rev.* **1994**, 11−19.

(2) (a) Nakako, H.; Nomura, R.; Tabata, M.; Masuda, T. *Macromolecules* **2001**, *34*, 1496−1502. (b) Nomura, R.; Fukushima, Y.; Nakako, H.; Masuda, T. *J. Am. Chem. Soc.* **2000**, *37*, 8830−8831. (c) Nakako, H.; Mayahara, Y.; Nomura, R.; Tabata, M.; Masuda, T. *Macromolecules* **2000**, *33*, 3978−3982. (d) Nakako, H.; Nomura, R.; Tabata, M.; Masuda, T. *Macromolecules* **1999**, *32*, 2861−2864.

(3) (a) Tabei, J.; Nomura, R.; Sanda, F.; Masuda, T. *Macromolecules* **2003**, *36*, 8603−8608. (b) Nomura, R.; Nishiura, S.; Tabei, J.; Sanda, F.; Masuda, T. *Macromolecules* **2003**, *36*, 5076−5080. (c) Nomura, R.; Tabei, J.; Nishiura, S.; Masuda, T. *Macromolecules* **2003**, *36*, 561−564. (d) Tabei, J.; Nomura, R.; Masuda, T. *Macromolecules* **2002**, *35*, 5405−5409. (e) Nomura, R.; Tabei, J.; Masuda, T. *Macromolecules* **2002**, *35*, 2955−2961. (f) Nomura, R.; Tabei, J.; Masuda, T. *J. Am. Chem. Soc.* **2001**, *123*, 8430−8431.

(4) (a) Deng, J.; Tabei, J.; Shiotsuki, M.; Sanda, F.; Masuda, T. *Macromolecules* **2004**, *37*, 1891−1896. (b) Deng, J.; Tabei, J.; Shiotsuki, M.; Sanda, F.; Masuda, T. *Macromol. Chem. Phys.* **2004**, *205*, 1103−1107.

(5) Schrock, R. R.; Osborn, J. A. *Inorg. Chem.* **1970**, *10*, 2339−2343.

MA049321B